Published in final edited form as:
Nat Genet. 2008 March ; 40(3): 290–298. doi:10.1038/ng.82.

MicroRNA Mirn140 modulates Pdgf signaling during palatogenesis

Johann K. Eberhart[1,*], **Xinjun He**[1,*], **Mary E. Swartz**[1], **Yi-Lin Yan**[1], **Hao Song**[1], **Taylor C. Boling**[1], **Allison K. Kunerth**[1], **Macie B. Walker**[2], **Charles B. Kimmel**[1], and **John H. Postlethwait**[1]

[1]Institute of Neuroscience, 1254 University of Oregon, Eugene, OR 97403, USA

Abstract

Disruption of signaling pathways such as those mediated by Shh or Pdgf causes craniofacial disease, including cleft palate. The role that microRNAs play in modulating palatogenesis, however, is completely unknown. We show, in zebrafish, that the microRNA Mirn140 negatively regulates Pdgf signaling during palatal development and we provide a mechanism for how disruption of Pdgf signaling causes palatal clefting. The *pdgf-receptor alpha* (*pdgfra*) 3' UTR contains a Mirn140 binding site functioning in the negative regulation of Pdgfra protein levels in vivo. Both *pdgfra* mutants and Mirn140-injected embryos share panoply of facial defects including clefting of the crest-derived cartilages that develop in the roof of the larval mouth. Concomitantly, the oral ectoderm beneath where these cartilages develop loses *pitx2* and *shha* expression. Mirn140 modulates Pdgf-mediated attraction of cranial neural crest cells to the oral ectoderm, where crest-derived signals are necessary for oral ectodermal gene expression. Both Mirn140 loss-of-function and *pdgfra* overexpression alters palatal shape and causes neural crest cells to accumulate around the optic stalk, a source of the ligand Pdgfaa. Conserved molecular genetics and expression patterns of *mirn140* and *pdgfra* suggest that their regulatory interactions are ancient methods of palatogenesis that provide a candidate mechanism for cleft palate.

Cleft palate and other craniofacial diseases are common in humans and have complex cellular and genetic etiologies. In amniotes, the palate serves to separate the nasal and oral cavities and is generated through an intricate series of morphogenic events that include early neural crest cell migration and cell-cell signaling during the formation of facial prominences, as well as later generation and fusion of palatal shelves. While later events involving palatal shelves have not been described in zebrafish, palatal precursors migrate both rostral and caudal to the eye to condense upon the oral ectoderm in amniotes[1] as well as zebrafish[2,3] and evidence continues to accumulate that the early signaling environment governing palatogenesis is also largely equivalent[3–6]. For instance, Hh signaling is crucial for palatogenesis in humans and zebrafish[3,4,7]. Zebrafish and amniotes also share expression patterns of palatogenic genes such as Shh[4,8], *Fgf8*[4,9,10] and *Pdgf receptor alpha (Pdgfra)*[11–13].

In mouse, the Pdgf family consists of four soluble ligands, Pdgfa, Pdgfb, Pdgfc, and Pdgfd as well as two receptor tyrosine kinases, Pdgfra and Pdgfrb[14]. Pdgf signaling regulates a myriad of biological processes as demonstrated by analyses of mouse Pdgf ligand and receptor mutants[14]. Mice null for *Pdgfra* have a facial clefting phenotype that includes cleft palate[12, 13]. This facial phenotype is fully recapitulated in mice doubly mutant for *Pdgfa* and *Pdgfc* 15. Most *Pdgfc* mutants have cleft palate[15] but *Pdgfa* mutants exhibit either severe phenotypes,

[2]Current address: Stowers Institute for Medical Research, 1000 E. 50th Street, Kansas City, MO 64110, USA
*These authors contributed equally.

dying before palatogenesis, or less severe phenotypes without cleft palate[16]. The inability to examine the severe phenotypic class for palatal defects precludes a clear understanding of how *Pdgfa* regulates palatogenesis. Whereas crest require the reception of Pdgf signaling during palatogenesis in mouse[13], the palatogenic cell behaviors regulated by Pdgf signaling and the modulation of Pdgf signaling during palatogenesis are unknown.

MicroRNAs (miRNAs) provide a unique mechanism for modulating signaling pathways[17–20]. Skeletogenic, including palatal, precursors express *mirn140* (*miR-140*) in teleosts[21] and amniotes[22–24], suggesting that Mirn140 may modulate signaling during palatogenesis across vertebrate species. Despite the function of miRNAs in development and the importance of neural crest in evolution and disease, no miRNA has yet been shown to regulate neural crest development or cellular behaviors.

One important neural crest cell behavior is their migration along highly stereotyped pathways to give rise to a diverse array of differentiated cell types. Across vertebrate species, crest cells at cranial levels migrate in one of three crest streams. Cells in the most anterior, or first, stream will migrate rostrally and caudally around the eye into the first pharyngeal arch and contribute to the jaw and palatal skeleton[5]. While research in zebrafish and amniotes have uncovered cues that regulate migration of cranial neural crest cells in all crest streams[25–27], nothing is known of what cues specifically guide neural crest-derived palatal precursors to the first pharyngeal arch.

Here, we show that Mirn140 attenuates Pdgf-mediated attraction during migration of neural crest-derived palatal precursors. Embryos injected with Mirn140 duplex and *pdgfra* mutants shared craniofacial phenotypes, including cleft palate and loss of oral ectoderm gene expression, suggesting an interaction between Mirn140 and *pdgfra*. Binding sites for Mirn140 are conserved in the 3' untranslated region (UTR) of *pdgfra* across vertebrate species and Mirn140 interacts with the 3'UTR of the *pdgfra* transcript to negatively-regulate Pdgfra protein production. Palatal precursors express both *mirn140* and *pdgfra* as they follow a migratory pathway delimited by expression of the ligand Pdgfaa. Attenuation of Pdgf signaling via Mirn140 is critical for rostrally migrating neural crest to migrate beyond the optic stalk, a Pdgfaa source, onward to the oral ectoderm, another Pdgfaa source. Our results demonstrate how delicately orchestrated modulation of Pdgf signaling regulates palatal morphogenesis.

RESULTS

Mirn140 and Pdgf signaling regulate palatal development in zebrafish

Skeletal precursors across vertebrate species express *mirn140*[21–24] and *mirn140* occupies the orthologous intron in *wwp2* of zebrafish, human, and other vertebrates (Supplementary Fig. 1), prompting the hypothesis that Mirn140 plays a conserved role in skeletogenesis across vertebrate species. To determine the *in vivo* role of Mirn140 during zebrafish skeletogenesis, we injected embryos with Mirn140 duplex. By 2 days post-fertilization (dpf), Mirn140 duplex injected embryos had a profound facial phenotype, including cranial hemorrhaging and a hypoplastic roof of the mouth (Fig. 1a,b,d, e). This hypoplasia suggested that the zebrafish skeletal palate was malformed and alcian/alizarin staining confirmed the presence of palatal defects, including cleft palate, in Mirn140 duplex injected embryos (Fig. 1g,h,j,k).

A clue to the target of Mirn140 during palatogenesis came from the fact that the array of facial defects seen in Mirn140 duplex injected embryos precisely phenocopy those observed in *pdgfra* ^{b1059} (*pdgfra*$^{-/-}$) mutants (Fig. 1c,f,i,l), identified in our forward genetic screen for craniofacial mutants (Fig. 1m). The *pdgfra*^{b1059} allele is likely hypomorphic since, unlike mouse *Pdgfra* mutants[12] and Mirn140 duplex injected zebrafish embryos (Supplementary Fig. 1), zebrafish *pdgfra* mutants had normal somites and were typically of similar size to their

wild-type siblings (data not shown). The molecular nature of the *pdgfra*^{b1059} allele is also consistent with *b1059* being hypomorphic. In *pdgfra*^{b1059} an I855N missense mutation is present near the activation loop of the second tyrosine kinase domain of the receptor. The sequence of this kinase core is highly conserved in Pdgfra across species and even across other related tyrosine kinase receptors such as Pdgfrb and Kit (Fig. 1m). Therefore the non-conservative hydrophobic to hydrophilic amino acid substitution is likely to attenuate, but not necessarily obliterate, receptor signaling. Pharmacologic inhibition of Pdgf receptor signaling, via Pdgfr inhibitor V, phenocopies the *b1059* allele and injection of *pdgfra* mRNA can rescue the palate of *b1059* embryos, providing confirmation that *b1059* lesions *pdgfra* (Supplementary Fig. 2). It is noteworthy that injection of *pdgfra* mRNA occasionally caused palatal defects in wild-type embryos (see below), suggesting that the overall level of Pdgf signaling must be strictly regulated for proper development of the palatal skeleton.

As in amniotes, the zebrafish palatal skeleton rests on the ectodermal roof of the oral cavity. In addition to their skeletal defect, the oral ectoderm of both Mirn140 duplex injected embryos and *pdgfra* mutant embryos failed to express regulatory genes such as *pitx2* (Fig. 2a–c) and *shha* (formerly called *shh*; Fig. 2d–f). The oral ectoderm is present, albeit misshapen, and its fate map is not altered as determined by anti-pan-cadherin antibody staining and Kaede photoconversion, respectively (Supplementary Fig 3). The oral ectoderm's morphological defect is not due to developmental delay because at all time points we've examined Mirn140 duplex injected embryos and *pdgfra* mutants display this defect (see Fig. 1e,f). The mechanism underlying this ectodermal defect is unclear, we do not detect elevated levels of cell death or loss of cell proliferation in the oral ectoderm (data not shown). In sum, the similarity of defects observed in Mirn140 duplex injected embryos and *pdgfra* mutants suggest a model where Mirn140 modulates Pdgf signaling, coordinating development of the palatal skeleton and the oral ectoderm.

Mirn140 regulates Pdgfra protein levels during palatogenesis

If Mirn140 modulates Pdgf signaling, Mirn140 binding sites should be present in the 3' UTR of one or more members of the Pdgf signaling pathway and their protein levels should be regulated by Mirn140. Sequence comparisons of the Pdgf signaling family revealed Mirn140 binding sites in the 3' UTR of *pdgfra* in all sequenced vertebrate genomes examined (Supplementary Table 1) and injection of Mirn140 duplex lowered Pdgfra protein levels (Fig. 3a). In contrast to *pdgfra*, the genes encoding zebrafish Pdgf ligands *pdgfaa*, *pdgfab*, *pdgfba*, *pdgfbb*, and *pdgfd* do not possess predicted Mirn140 binding sites. Although *pdgfc* has a Mirn140 binding site, the craniofacial region expresses *pdgfc* at 30 hpf, after the time we show that Mirn140 has its effects on palatogenesis (see below). An alternative hypothesis, that Mirn140 acts via inhibition of *hdac4*, as in mouse tissue culture cells[24], is unlikely. Zebrafish *hdac4* does not have a candidate Mirn140 binding site, nor does the scheduling or quantity of bone in Mirn140 over-expression or knockdown animals change as predicted by the tissue culture studies, suggesting that *hdac4* is not a significant *in vivo* target of Mirn140 in zebrafish embryos. These results suggest that Mirn140 has its effects on palatal morphogenesis through inhibition of Pdgfra.

To directly test whether Mirn140 negatively regulates Pdgfra via the 3'UTR of *pdgfra*, we fused *GFP* to the 3'UTR of zebrafish *pdgfra* (GFP-*pdgfra*, Fig. 3b). Embryos co-injected with Mirn140 duplex and GFP-*pdgfra* lost GFP fluorescence (Fig. 3c–e,g), compared to controls. In contrast to GFP-*pdgfra*, reporter constructs fusing *GFP* to the 3'UTR of *nog3*, lacking a Mirn140 binding site, failed to respond to Mirn140 duplex (data not shown). To determine the extent of Pdgfra modulation via Mirn140, we injected embryos with *mirn140* morpholino and assayed Pdgfra protein levels and expression of the *GFP-pdgfra* reporter. Knockdown of endogenous Mirn140 elevated Pdgfra protein levels (Fig. 3a) and GFP fluorescence compared

to controls (Fig. 3c,f,g). These experiments show that the 3'UTR of *pdgfra* is a target of Mirn140.

Because miRNAs have many predicted targets [28], we co-injected Mirn140 duplex along with *pdgfra* mRNA lacking the Mirn140 binding site (*pdgfra**) to test if the effects of Mirn140 on craniofacial development are mediated by Pdgfra. Co-injection of *pdgfra** mRNA rescued Mirn140 duplex injected embryos (Fig. 3h–k), indicating that the cleft palate phenotype of Mirn140 duplex injected embryos is primarily due to loss of Pdgf signaling.

Our results show that Mirn140 attenuates Pdgf signaling and that Pdgf signaling is required for palatogenesis, but the cellular events mediated by Pdgf signaling during palatogenesis are unknown. Examining neural crest migration in mouse *Pdgfra* mutants uncovered no defect[13], yet early phenotypic changes in zebrafish postmigratory crest (described below) were suggestive that migration of palatal precursors was abnormal. Therefore, we examined the expression of *mirn140* and Pdgf signaling components during crest migration to elucidate how Pdgf signaling is involved in neural crest cell migration.

Consistent with previous reports[11], we found that most, if not all, cranial neural crest cells express *pdgfra*. Crest-derived palatal precursors, fate mapped in previous studies[3,4], migrate around the eye to reach the oral ectoderm and the subset of these crest cells migrating rostrally to the eye must additionally migrate around the optic stalk (see below). Both rostrally and caudally migrating crest cells express *pdgfra* throughout migration to the oral ectoderm (Fig. 4a,c,e,g). This expression pattern suggests that Pdgfra mediates migration of palatal precursors to the oral ectoderm.

To determine what ligand Pdgfra utilizes during crest cell migration, we cloned and surveyed the expression of the zebrafish homologues of *Pdgfa* and *Pdgfc*, because mice doubly mutant for these genes recapitulate the mouse *Pdgfra* mutant phenotype[12,15]. The zebrafish genome (http://www.ensembl.org/Danio_rerio/index.html) contains a single copy of *pdgfc* and duplicates of *pdgfa*, we designate these *pdgfaa* (formerly called *pdgf-a*[29]) and *pdgfab*. We found that only *pdgfaa* has spatiotemporal expression appropriate for gene encoding a candidate crest cell guidance molecule. Just before migration initiates, the midbrain expresses *pdgfaa* in a pattern that predicts the location of *pdgfra*-expressing palatal skeleton precursors four hours later (Fig. 4a–d). Expression is dynamic, and shifts to include the optic stalk and oral ectoderm as rostral crest cells migrate around the eye and optic stalk to reach the oral ectoderm (Fig. 4e–h). Well after palatogenic crest have reached the oral ectoderm, the optic stalk and oral ectoderm maintain expression of *pdgfaa* (Supplementary Fig. 4) and other Pdgf ligands begin to be expressed in the pharyngeal arches (Supplementary Fig. 4). These results are consistent with Pdgfaa acting as an attractant cue guiding palatal precursors to the oral ectoderm.

Because our reporter constructs demonstrated that Mirn140 functions by negatively regulating Pdgfra levels, we expect to see *mirn140* and *pdgfra* co-expressed. RT-PCR detected *mirn140* transcripts as early as 1 hpf and throughout crest cell migration (Fig. 4i) and in situ hybridization demonstrated that these transcripts were distributed broadly as late as 24 hpf (Fig. 4j). Following crest cell migration, transcripts for *mirn140* became localized to skeletogenic crest (Fig. 4k,l), similar to the later expression of *pdgfra*[11]. This expression profile of *mirn140* supports the conclusion that it modulates Pdgfra levels during palatal development, including crest cell migration.

Together, our results suggest the hypothesis that Mirn140, acting via Pdgfra, modulates Pdgf-mediated attraction of palatal precursor cells, which is required for correct migration.

Pdgf signaling is an attractant cue for palatal precursor cells

Our hypothesis predicts that palatal precursor migration[3,4] will be disrupted in *pdgfra* mutants. Analyses in *sox10:EGFP* transgenic embryos show that palatal precursor cells[JP1] normally disperse rapidly rostrally and caudally around the eye to reach the oral ectoderm, where they condense (Supplementary Movie 1). Rostrally migrating cells must migrate around the optic stalk before reaching the oral ectoderm (Fig. 5a, Supplementary Movie 1). In *pdgfra* mutants, palatal precursors did not disperse but rather stayed tightly grouped together (Fig. 5b). Additionally, rostral crest did not migrate around the optic stalk (Fig. 5b), and most crest cells never reached the oral ectoderm (Supplementary Movie 2). We did not detect elevated levels of cell death in the crest cells or their migratory pathway during crest migration (data not shown), although it remains a possibility that cell death does occur at a later time. Crest cells that reached the oral ectoderm in *pdgfra* mutants did so via a circuitous route, avoiding a cell-free region normally invaded by crest (Supplementary Fig. 5). In contrast to palatal precursors, most other neural crest cells in *pdgfra*$^{-/-}$*;sox10:EGFP* embryos migrated appropriately (Supplementary Fig. 5), similar to findings in mouse[13]. Hence, a subpopulation of neural crest cells, namely palatal precursors, requires Pdgfra function for proper migration.

Our hypothesis also predicts that both *pdgfaa* loss-of-function and Mirn140 overexpression should result in palatal precursor migration defects as observed in *pdgfra* mutants. Similar to *pdgfra* mutants, neural crest cells in *pdgfaa* morpholino injected or Mirn140 duplex injected, *sox10:EGFP* transgenic embryos failed to disperse and rostral crest cells stopped migrating at the optic stalk (Fig. 5c,d) resulting in clefting or reduction in the palatal skeleton (Fig. 1h,k; Supplementary Fig. 6). This effect on migration of *pdgfra*-expressing crest cells (Fig. 5e,f, arrows) in Mirn140 duplex injected embryos was not through loss of *pdgfra* transcripts, suggesting that Mirn140 attenuates Pdgf signaling by blocking Pdgfra translation. Collectively, we have shown that loss of Pdgf signaling either by blocking the ligand, by mutating the receptor, or by Mirn140 overexpression, results in the failure of palatal precursors to reach the oral ectoderm.

Phenotypes resulting from loss of Pdgf signaling and our expression analyses are consistent with Pdgf signaling being a positive guidance cue for cranial neural crest. To directly test the nature of Pdgf signaling during crest migration, we implanted beads soaked in PDGFA or BSA (bovine serum albumin), as a negative control, into *pdgfaa* morpholino injected *sox10:EGFP* transgenic embryos. Neural crest cells accumulated next to PDGFA beads, but not BSA beads (Fig. 5g–i, arrows), demonstrating that PDGFA is a positive cue, probably a chemoattractant as it is in oligodendrocyte migration[30], that guides crest to the oral ectoderm.

Loss of Pdgf signaling causes defects in both cranial neural crest cell migration and oral ectodermal gene expression, yet we never detected *pdgfra* transcripts in the oral ectoderm. In mouse, Pdgfra function is required in neural crest for proper palatogenesis[13]. Additionally, interspecific neural crest transplantation in avian species has shown that the oral ectoderm responds to crest-derived signals[31], predicting that loss of oral ectodermal gene expression in *pdgfra* mutants is secondary to the failure of crest to reach the oral ectoderm. We tested both these predictions by transplanting *pdgfra*$^{+}$ crest into *pdgfra*$^{-/-}$ hosts and assaying neural crest migration and oral ectoderm gene expression. Neural crest cells from *pdgfra*$^{+}$*;sox10*:EGFP donors dispersed and migrated to the oral ectoderm normally in *pdgfra*$^{-/-}$ hosts (Fig. 6a,b). Not only did transplanted *pdgfra*$^{+}$ crest restore the palatal skeleton (Fig. 6e), but it also rescued gene expression (Fig. 6f) in the *pdgfra*$^{-/-}$ oral ectoderm. These transplants frequently contain contaminant, non-neural crest cells, yet these contaminant cells were typically distant from the oral ectoderm (Fig. 6d, asterisks) and thus unlikely to influence oral ectodermal development. Therefore, a crest migration defect is the primary cause of both the palatal skeleton and oral ectodermal phenotypes observed in embryos lacking functional Pdgf signaling.

Mirn140 is necessary for rostrally migrating neural crest cells to reach the oral ectoderm

We have shown that Mirn140 negatively regulates Pdgf signaling, which is required for neural crest cells to migrate to the oral ectoderm and alter oral ectodermal gene expression. To further probe the normal function of Mirn140, we utilized morpholinos to knock down Mirn140 activity.

Loss of Mirn140 activity resulted in dramatically elevated levels of Pdgfra protein (Fig. 3a) and caused alteration in the shape of the palatal skeleton (Fig. 7a). Co-injection of Mirn140 duplex rescues this palatal phenotype, showing specificity of the morpholino (Fig. 7a). Normally in zebrafish, caudally migrating neural crest cells give rise to the lateral palatal skeleton, while rostrally migrating cells fill in the medial palatal skeleton[3]. Therefore, shape change after Mirn140 knockdown could be due to changes in the relative contributions of caudal versus rostral crest cells to the palatal skeleton.

Rostrally migrating crest cells must pass the optic stalk, a Pdgfaa source, to reach the oral ectoderm. Therefore, elevating Pdgf signaling by injections of either *mirn140* morpholino or *pdgfra** mRNA, which lacks the Mirn140 binding site, may alter the number of rostral crest cells migrating past the optic stalk. In *sox10:EGFP* transgenic embryos, we found that many crest cells had migrated past the optic stalk (Fig. 7f, os) to the oral ectoderm by 24 hpf. However, after injection with either *mirn140* morpholino or *pdgfra** mRNA neural crest cells enveloped the optic stalk, yet few had migrated on to the oral ectoderm (Fig. 7g,h). The palatal skeleton's morphology was altered in *mirn140* morpholino injected embryos (Fig. 7j), but appeared fairly normal in *pdgfra** injected embryos (Fig. 7k). This difference could be due to the labile nature of mRNA allowing the embryo to recover by 6 days post injection. We conclude that elevation of Pdgf signaling causes alterations in the shape of the palatal skeleton by reducing the number of rostrally migrating crest cells that reach the oral ectoderm.

Discussion

Here we show that precise control of Pdgf signaling is crucial for at least two separate events in crest migration. First, Pdgf signaling is necessary for neural crest cell dispersion (Fig. 8a). Most or all palatal precursors do not disperse if Pdgf signaling levels are low, whether by *pdgfra* mutation, *pdgfaa* morpholino injection, or Mirn140 duplex injection. How dispersion may be interrelated with migration remains to be elucidated, but caudally migrating crest cells are initially located very close to the oral ectoderm. Therefore, proper dispersion could play a large part in the migration of caudal cells to the oral ectoderm.

Our results show, secondly, that modulated Pdgf signaling is critical for rostrally migrating cells to reach the oral ectoderm. In embryos with reduced Pdgf signaling, rostrally migrating neural crest cells do not migrate around the optic stalk, whereas in embryos with elevated Pdgf signaling, crest cells encircle the optic stalk, but few migrate on to the oral ectoderm. The optic stalk continues to express *pdgfaa* while palatal precursors migrate on to the oral ectoderm. Since Pdgfaa is an attractant cue for neural crest cells, there would normally be little reason for crest to leave the optic stalk unless Pdgf signaling was attenuated. In addition to the facial skeleton, crest cells normally contribute to structures associated with optic stalk derivatives [32]. We propose a model where subtle stoichiometric differences between Mirn140 and *pdgfra* mRNA levels mediate the choice of neural crest cells to stay at the optic stalk or move on to the oral ectoderm to form the palatal skeleton (Fig. 8b).

Mirn140-mediated attenuation of Pdgf signaling may also play a significant role in the development of tissues outside the craniofacial skeleton. Mirn140 injected embryos have defects in cardiac and somite development as well as body axis elongation (see Supplementary Fig. 1). Mouse *Pdgfra* mutants share defects in all these systems but, while zebrafish *pdgfra*

mutants do have cardiac defects, somite development and body axis elongation appear fairly normal (data not shown). The similarities in phenotypes between mouse *Pdgfra* mutants and Mirn140 injected zebrafish suggests conservation of Pdgfra function across vertebrate species, even though the presumptive hypomorphic *pdgfra*^{b1059} allele does not cause defects in all these developmental systems. Since, it is possible that Mirn140 regulates multiple signaling pathways, analyses in zebrafish null *pdgfra* alleles, yet to be identified, will be necessary to determine the full extent of conservation of Pdgfra function.

Our findings suggest that miRNA-mediated modulation of Pdgfra signaling may have evolutionary significance. In amniotes, snout length is associated with the relative contributions of the frontonasal prominence, derived from rostrally migrating cells, and the maxillary prominence, derived from caudally migrating cells, to the facial skeleton[33,34]. Therefore, the evolution of skull morphology could utilize miRNAs, in particular Mirn140, to tweak the number of crest cells arriving at an individual prominence within the first pharyngeal arch.

Cranial neural crest cells migrate to the pharyngeal arches in three crest streams, with the first stream populating the first pharyngeal arch,[2] and yet no guidance cue responsible for the migration of any individual stream has been discovered. We show that loss of Pdgf signaling disrupts the migration of a subpopulation of first stream crest, those destined for the zebrafish palate. As in mouse[13], all three crest streams express *pdgfra*. Hence, it is the expression of *pdgfaa*, encoding a ligand for Pdgfra, which provides the mechanism for Pdgf signaling to specifically guide palatal precursors. As crest cells migrate *pdgfaa* expression consistently and specifically predicts the pathway to be taken by palatal precursors. We propose that the restricted expression of *pdgfaa* attracts only palatal precursors since Pdgf signaling acts at short range[14] and, therefore, cranial crest in more posterior streams would not receive Pdgf signaling. The same tissues that express *pdgfaa* in zebrafish also express *Pdgfa* in amniotes [35–37], consistent with the possibility that Pdgfa signaling plays similar roles in zebrafish and amniotes. Crest migration defects have not been described in mouse *Pdgfra* or *Pdgfa* mutants[12,13,16], this could be due to species-specific developmental differences or to improved visualization of crest in zebrafish. It will be of great interest to determine if palatal precursor migratory defects are evident in mouse *Pdgfra* and *Pdgfa* mutants, although conditional mutation of *Pdgfa* would be necessary to overcome the early death of severely effected *Pdgfa* mutant mice[16].

Further exploration of how microRNAs and other factors modulate signaling pathways such as Pdgf during palatogenesis will assuredly continue to provide insights into the cause of, and possible treatments for, human craniofacial disease.

Materials and Methods

Oligonucleotides

All oligonucleotides are listed in Supplementary Table 2.

Zebrafish care and use

The *b1059* mutant allele was obtained via ENU mutagenesis[39] in an AB background and was out-crossed to a WIK background for genetic mapping. PCR-based microsatellite mapping placed the *b1059* allele in a 1.4 cM interval of LG20, between microsatellite markers z14542 (7 cross overs/434 meioses) and z20582 (2 cross overs/434 meioses), which contains 23 known genes including *pdgfra*. Given the phenotypic similarities of mouse *Pdgfra* mutants and *b1059* mutants, *pdgfra* was an excellent candidate for the gene lesioned in *b1059* mutants. Sequence analysis of *pdgfra* in wild-type and *b1059* embryos revealed an adenosine-to-thymidine nucleotide change resulting in an I855N missense mutation, thus placing a charged

residue in the hydrophobic core of the kinase C-lobe in the second tyrosine kinase domain of the receptor. *pdgfra*^{b1059} mutants were identified by either phenotype or PCR amplification using dCAPs primers[40], forward: 5' TGTCTCCAAAGGAAGCGTG 3' and reverse: 5' ACCGAGAGAGAAGATCTCCCATAACTAG 3', followed by digestion with SpeI, resulting in a wild-type fragment of 263 bp and a *b1059* fragment of 239 bp. Throughout the text we use *pdgfra*$^{+}$ to refer to embryos with either *pdgfra*$^{+/-}$ or *pdgfra*$^{+/+}$ genotypes.

All embryos were raised and cared for using established protocols[39] with IACUC approval. *Tg(fli1:EGFP)*^{y1} transgenic embryos express GFP in neural crest cells shortly after the onset of migration, and in the vasculature [41], while *Tg(-4.9sox10:EGFP)*^{ba2} transgenic embryos express GFP in neural crest prior to the onset of migration[3]; here they are called *fli1:EGFP* and *sox10:EGFP*, respectively, through the text. We used heterozygous *sox10:EGFP* transgenics for our analyses, because homozygous embryos can have craniofacial defects[3]. Embryos were treated with 0.5 μM Pdgfr inhibitor V (Calbiochem) from 10 hpf- 4 dpf and Kaede photoconversion was carried out as described previously[4].

Morpholino and RNA injection

Gene Tools (Philomath, OR, USA, http://www.gene-tools.com) supplied morpholino oligonucleotides (MOs) with the sequences: *mirn140* MO (mature), 5'-CTACCATAGGGTAAAACCACTG-3'; *mirn140* MO (Dicer inhibitor), 5'-GACGTAACCTACCATAGGGTAAAACCACTGA-3'; *p53* MO, 5'-GCGCCATTGCTTTGCAAGAATTG-3' [42] *pdgfaa* I1E2 (splice inhibitor) 5' GGAATTGGTGCTTCCTGTTAAAGA 3' and *pdgfaa* I2E3 (splice inhibitor) 5' CCTCCAGCACTTCATTCTCTGCAAC.

We injected one or two-cell stage zebrafish embryos with approximately 3 nl of morpholinos: 0.4 mM *pdgfaa*, 1.2 mM mature *mirn140*, or 0.6 mM Dicer inhibitor *mirn140*. Injecting higher concentrations of *pdgfaa* morpholino resulted in embryos with disrupted body axes, consistent with *pdgfaa* playing a role in gastrulation movements[43]. To control for the effects of nonspecific cell death, we co-injected either *pdgfaa* morpholino or *mirn140* morpholino (Dicer inhibitor, 1.2 mM) with *p53* morpholino (0.3 mM)[44].

Integrated DNA Technology (Coralville, IA, USA, http://www.idtdna.com) supplied RNA oligonucleotides with the sequences: Mirn140, 5'-CAGUGGUUUUACCCUAUGGUAG-3'; Mirn140 mismatch, 5'-CACACCAAGAACCCUAUGGUAG-3'; Mirn140* (the complementary natural strand), 5'-UACCACAGGGUAGAACCACGGAC-3'. To make 50 μM working stocks, 10 μL of 100 μM Mirn140 or Mirn140 mismatch plus 10 μL of 100 μM Mirn140 * were mixed together, boiled briefly to denature, and then slowly cooled to 4°C and stored at −80°C until injection. Embryos were injected with 3 nl of this 50 μM working stock or a 25 μM dilution of this stock, with identical results. To rescue the cleft palate phenotype in Mirn140 duplex injected embryos (25 uM), we co-injected *mirn140* MO (Dicer inhibitor, 1.2 mM).

Reporter constructs

The primers pdgfraUTR-F (5'-TCTGCGTCATCTTGTCACTTTTTCTTCAC-3') and pdgfraUTR-R (5'-AACACAGCCATTTTCTTCATTTTAGGAC-3') amplified a 653 bp long fragment from genomic DNA containing the *pdgfra* 3' untranslated region (UTR), which was inserted into the pCR4-TOPO vector (Invitrogen, Carlsbad, CA, USA, http://www.invitrogen.com). To fuse GFP with the *pdgfra* 3'UTR, we used NotI and SpeI enzymes to liberate the 3'UTR region of *pdgfra* gene from pCR4-TOPO and NotI and XhoI to extract *GFP* from pEGFP-N3 (Clontech, Mountain View, CA, USA, www.clontech.com).

We ligated the fragments into PCRII-TOPO (Invitrogen) between SpeI and XhoI sites, to make *GFP-pdgfra*. To make mRNA, the vector was linearized with SpeI.

Co-injections were accomplished by double injection, first by injecting 0.6 mM Dicer inhibitor *mirn140* MO or 25 μM Mirn140 duplex, and then by injecting 250 ng/μL of the synthetic GFP-*pdgfra* UTR mRNA. *GFP-nog3* UTR construct was made similarly to the *GFP-pdgfra* UTR with the primers: nog3-F (5'-GAAATAAGCTCCGCACTCATCCTCACAT-3') and nog3-R (5'-TCCATTCCCCTTATATTTACAGCACACCA-3'), amplifying a 504 bp fragment containing the *nog3* 3'UTR.

We amplified full-length *pdgfra* lacking the Mirn140 binding site (*pdgfra**) using primers pdgfra-F (5'-TCATGTTCCCGGTGCTGCC-3') and pdgfra-R (5'-GGGCTCCATAAGACTGAGGTGAAG-3'). The resulting 3418 bp PCR product was ligated into pCR4-TOPO. To make mRNAs, plasmid was linearized with SpeI and about 1 μg of purified linear template was transcribed by T7 RNA polymerase using mMessenger mMachine kit (Ambion, Austin, TX, USA, http://ambion.com) at 37 °C for 2 h. mRNAs were purified with RNA clean up kit (Zymo Research, Orange County, CA, http://www.zymoresearch.com) and diluted to 15 μL with nuclease-free water. We used this truncated mRNA for all of our *pdgfra* mRNA injections, including rescue of $pdgfra^{b1059}$ mutants. The truncated *pdgfra* mRNA only alters the levels of Pdgfra protein produced from the mRNA and therefore does not alter the interpretation of our $pdgfra^{b1059}$ rescue experiment.

Cloning and in situ hybridization

Primers for generating PCR products containing the full open reading frame of Pdgf family members and *mirn140* are: *pdgfra* (Ensembl Gene ID ENSDARG00000030379) forward 5' TCATGTTCCCGGTGCTGCC 3' and reverse 5' GGGCTCCATAAGACTGAGGTGAAG, *pdgfaa* (Ensembl Gene ID ENSDARG00000030379) forward 5' TGGGACACTTTTGGACCACAGG 3' and reverse 5' TCGTTTTTCAGGCTGTCGTTG 3', *pdgfab* (Ensembl Gene ID ENSDARG00000058424) forward 5' TGACATTGGAAGGAGATGAGAACC 3' and reverse 5' TTATTGAATATCCTTGTTGATCAGTGC 3' and *pdgfc* (Genbank accession XM 683962.2) forward 5' CCAAATGATTCCGTTGCTTCTG 3' and reverse 5' GCGTCTTCTCTCTGGGACTGATT 3'. A 902 bp fragment of *pri-mirn140* was isolated from 24 hpf embryo cDNA library by the primers primiR140-F (5'-GCAAGTCAAACCCTGTAGCATCCCGTT-3') and primiR140-R (5'-GCGAGCCGATAGAGCGATTGTTT-3'). *mirn140* (dre-mir-140 primary transcript, EU116273) was cloned by RT-PCR and 3' RACE from 24 hpf zebrafish embryo cDNA. PCR products were cloned in pCR4-TOPO (Invitrogen). ClustalX alignment confirmed our Pdgf orthologue assignments. Capped mRNA was synthesized using the mMessage mMachine kit (Ambion, Austin, TX).

Integrated DNA Technology synthesized *mirn140* LNA (Locked Nucleic Acid) probe (5'-CtACcATaGGgTAaAAcCAcTG-3', lowercase nucleotides represent LNA nts) with 3' end Digoxigenin-labeling. Probe was diluted to 0.5 μM in hybridization buffer (50% formamide, 2XSSC, 0.3% Tween-20, 0.5 mg/mL baker's yeast RNA and 0.05 mg/mL heparin). *In situ* hybridization occurred at 43 °C on whole mounted embryos and frozen sections following protocols provided by Exiqon (Woburn, MA, USA, http://exiqon.com). In situ hybridizations utilizing *mirn140* LNA yielded results identical to *pri-mirn140* probe (not shown). Conventional *in situ* hybridization with digoxigenin-labeled RNA probes utilized a protocol similar to that for the LNA probe, but at a hybridization temperature of 68 °C. Cutting circular plasmid with NotI and synthesizing RNA with T3 polymerase generated antisense *pdgfra*, *pdgfaa*, and *pdgfc* riboprobes, whereas cutting with SpeI and synthesizing with T7 polymerase produced *pdgfab* and *pri-mirn140* riboprobe. *pitx2* and *shh* riboprobes have been described[4].

Accession numbers for sequences used in this work: *pdgfaa*, NM_194426; *pdgfab*, NM_001076757; *pdgfb*, ESTs DV584985 and EB884207; *pdgfc*, XM_683962 and EST EH559317; *pdgfd*, XM_001333193; *pdgfra*, NM_131459 ENSDART00000011915;

Cartilage staining

Six day postfertilization zebrafish embryos were stained with Alcian Blue and flat mounted[45].

Cell transplants and bead implants

For all transplants, donors were injected with 10,000 MW Alexa 568 dextran, labeling all cells. Shield stage transplants were carried out as described elsewhere[4].

Affi-gel blue gel (BioRad) was incubated overnight at 4° with 10 μg/ml rat recombinant Pdgfaa (R&D Systems) or BSA (Sigma). Individual Affi-gel beads from the gel were inserted into *pdgfaa* morpholino injected embryos at 12 hpf and implanted embryos were imaged at 20 hpf.

Time-lapse analysis, confocal microscopy, and figure processing

Confocal z-stacks were collected on a Zeiss LSM Pascal. Images were processed in Adobe Photoshop CS and Adobe Illustrator. Recordings, 15 min/frame, and confocal analysis of transgenic embryos were performed according to established protocols[4]. To quantitate GFP levels, pixels of individual layers were selected by setting Fuzziness level to 170. The histogram function was then used to calculate the number and standard deviations of green pixels for each fish.

Western blotting

Immunoblotting used the Upstate (http://www.upstate.com) protocol with minor modifications. Proteins extracted from thirty 24 hpf fish were separated by SDS polyacrylamide gel electrophoresis and transferred to a nitrocellulose membrane using 3% blocking solution. The blot was probed with anti-human PDGFRA antibody (catalog# 07–276, Upstate) and anti-mouse ACTIN antibody (product# A4700, Sigma, St. Louis, MO, USA, http://www.sigmaaldrich.com) using HRP-conjugated secondary antibodies, anti-rabbit (catalog # AP132P) (Chemicon, Temecula, CA, USA, http://www.chemicon.com) and anti-mouse (AP124P) (Chemicon). Protein blots were visualized by ECL Western Blotting Detection System (Catalog # RPN2132, Amersham, Piscataway, NJ, USA. http://www.amersham.com).

Statistical Analysis

JMP version 5.1 software (SAS Institute, Cary, NC) was used for oneway ANOVA.

Supplementary Material

Refer to Web version on PubMed Central for supplementary material.

Acknowledgements

We thank Ruth BreMiller for help with histology and John Dowd and the University of Oregon Zebrafish Facility for animal care. Morpholinos were provided by John Moulton at Gene Tools as part of Multi-Blocker field testing. This work was supported by the National Center for Research Resources (5R01RR020833 to JHP) and National Institutes of Health (P01 HD22486 to CBK and JHP and 5 K99 DE018088 to JKE); the contents of this study are solely the responsibility of the authors and do not necessarily represent the official views of NCRR or NIH.

References

1. Osumi-Yamashita N, Ninomiya Y, Doi H, Eto K. The contribution of both forebrain and midbrain crest cells to the mesenchyme in the frontonasal mass of mouse embryos. Developmental Biology 1994;164:409–419. [PubMed: 8045344]
2. Trainor PA, Melton KR, Manzanares M. Origins and plasticity of neural crest cells and their roles in jaw and craniofacial evolution. International Journal of Developmental Biology 2003;47:541–553. [PubMed: 14756330]
3. Wada N, et al. Hedgehog signaling is required for cranial neural crest morphogenesis and chondrogenesis at the midline in the zebrafish skull. Development 2005;132:3977–3988. [PubMed: 16049113]
4. Eberhart JK, Swartz ME, Crump JG, Kimmel CB. Early Hedgehog signaling from neural to oral epithelium organizes anterior craniofacial development. Development 2006;133:1069–1077. [PubMed: 16481351]
5. Trainor PA, Krumlauf R. Hox genes, neural crest cells and branchial arch patterning. Current Opinion in Cell Biology 2001;13:698–705. [PubMed: 11698185]
6. Hilliard SA, Yu L, Gu S, Zhang Z, Chen YP. Regional regulation of palatal growth and patterning along the anterior-posterior axis in mice. Journal of Anatomy 2005;207:655–667. [PubMed: 16313398]
7. Roessler E, et al. Mutations in the human sonic hedgehog gene cause holoprosencephaly. Nature Genetics 1996;14:357–360. [PubMed: 8896572]
8. Hu D, Helms JA. The role of sonic hedgehog in normal and abnormal craniofacial morphogenesis. Development 1999;126:4873–4884. [PubMed: 10518503]
9. Riley BM, et al. Impaired FGF signaling contributes to cleft lip and palate. Proceedings of the National Academy of Sciences USA 2007;104:4512–4517.
10. Bachler M, Neubüser A. Expression of members of the Fgf family and their receptors during midfacial development. Mechanisms of Development 2001;100:313–316. [PubMed: 11165488]
11. Liu L, Chong SW, Balasubramaniyan NV, Korzh V, Ge R. Platelet-derived growth factor receptor alpha (pdgfr-alpha) gene in zebrafish embryonic development. Mechanisms of Development 2002;116:227–230. [PubMed: 12128230]
12. Soriano P. The PDGF alpha receptor is required for neural crest cell development and for normal patterning of the somites. Development 1997;124:2691–2700. [PubMed: 9226440]
13. Tallquist MD, Soriano P. Cell autonomous requirement for PDGFRalpha in populations of cranial and cardiac neural crest cells. Development 2003;130:507–518. [PubMed: 12490557]
14. Betsholtz C, Karlsson L, Lindahl P. Developmental roles of platelet-derived growth factors. BioEssays 2001;23:494–507. [PubMed: 11385629]
15. Ding H, et al. A specific requirement for PDGF-C in palate formation and PDGFR-alpha signaling. Nature Genetics 2004;36:1111–1116. [PubMed: 15361870]
16. Boström H, et al. PDGF-A signaling is a critical event in lung alveolar myofibroblast development and alveogenesis. Cell 1996;85:863–873. [PubMed: 8681381]
17. Hornstein E, Shomron N. Canalization of development by microRNAs. Nature Genetics 2006;38:S20–S24. [PubMed: 16736020]
18. Lee CT, Risom T, Strauss WM. MicroRNAs in mammalian development. Birth Defects Research. Part C, Embryo Today 2006;78:129–139.
19. Shalgi R, Lieber D, Oren M, Pilpel Y. Global and local Architecture of the mammalian microRNA-transcription factor regulatory network. PLoS Computational Biology 2007;3:e131. [PubMed: 17630826]
20. Song L, Tuan RS. MicroRNAs and cell differentiation in mammalian development. Birth Defects Research. Part C, Embryo Today 2006;78:140–149.
21. Wienholds E, et al. MicroRNA expression in zebrafish embryonic development. Science 2005;309:310–311. [PubMed: 15919954]
22. Ason B, et al. Differences in vertebrate microRNA expression. Proceedings of the National Academy of Sciences USA 2006;103:14385–14389.

23. Darnell DK, et al. MicroRNA expression during chick embryo development. Developmental Dynamics 2006;235:3156–3165. [PubMed: 17013880]
24. Tuddenham L, et al. The cartilage specific microRNA-140 targets histone deacetylase 4 in mouse cells. FEBS Letters 2006;580:4214–4217. [PubMed: 16828749]
25. Gammill LS, Gonzalez C, Bronner-Fraser M. Neuropilin 2/semaphorin 3F signaling is essential for cranial neural crest migration and trigeminal ganglion condensation. Developmental Neurobiology 2007;67:47–56. [PubMed: 17443771]
26. McLennan R, Kulesa PM. In vivo analysis reveals a critical role for neuropilin-1 in cranial neural crest cell migration in chick. Developmental Biology 2007;301:227–239. [PubMed: 16959234]
27. Yu HH, Moens C. Semaphorin signaling guides cranial neural crest cell migration in zebrafish. Developmental Biology 2005;280:373–378. [PubMed: 15882579]
28. Griffiths-Jones S, Grocock RJ, van Dongen S, Bateman A, Enright AJ. miRBase: microRNA sequences, targets and gene nomenclature. Nucleic Acids Res 2006;34:D140–D144. [PubMed: 16381832]
29. Liu L, Korzh V, Balasubramaniyan NV, Ekker M, Ge R. Platelet-derived growth factor A (pdgf-a) expression during zebrafish embryonic development. Development Genes and Evolution 2002;212:298–301. [PubMed: 12211169]
30. Zhang H, Vutskits L, Calaora V, Durbec P, Kiss JZ. A role for the polysialic acid-neural cell adhesion molecule in PDGF-induced chemotaxis os oligodendrocyte precursor cells. Journal of Cell Science 2004;117:93–103. [PubMed: 14627627]
31. Schneider RA, Helms JA. The cellular and molecular origins of beak morphology. Science 2003;299:565–568. [PubMed: 12543976]
32. Sadaghiani B, Thiebaud CH. Neural crest development in the *Xenopus laevis* embryo, studied by interspecific transplantation and scanning electron microscopy. Developmental Biology 1987;124:91–110. [PubMed: 3666314]
33. Osumi-Yamashita N, Ninomiya Y, Doi H, Eto K. The contribution of both forebrain and midbrain crest cells to the mesenchyme in the frontonasal mass of mouse embryos. Developmental Biology 1994;164:409–419. [PubMed: 8045344]
34. Brugmann SA, et al. Wnt signaling mediates regional specification in the vertebrate face. Development 2007;134:3282–3295.
35. Orr-Urtreger A, Lonai P. Platelet-derived growth factor-A and its receptor are expressed in separate, but adjacent cell layers of the mouse embryo. Development 1992;115:1045–1058. [PubMed: 1451656]
36. Ho L, Symes K, Yordan C, Gudas LJ, Mercola M. Localization of PDGF A and PDGFR alpha mRNA in Xenopus embryos suggests signalling from neural ectoderm and pharyngeal endoderm to neural crest cells. Mechanisms of Development 1994;48:165–174. [PubMed: 7893600]
37. Tallquist MD, Weismann KE, Hellström M, Soriano P. Early myotome specification regulates PDGFA expression and axial skeleton development. Development 2000;127:5059–5070. [PubMed: 11060232]
38. Foppiano S, Hu D, Marcucio RS. Signaling by Bone Morphogenetic Proteins directs formation of an ectodermal signaling center that regulates craniofacial development. Developmental Biology. 2007in press
39. Westerfield, M. The Zebrafish Book; A guide for the laboratory use of zebrafish (Brachydanio rerio). 1993.
40. Neff MM, Neff JD, Chory J, Pepper AE. dCAPS, a simple technique for the genetic analysis of single nucleotide polymorphisms: experimental applications in Arabidopsis thaliana genetics. The Plant Journal 1998;14:387–392. [PubMed: 9628033]
41. Lawson N, Weinstein BM. In vivo imiagining of embryonic vascular development using transgenic zebrafish. Developmental Biology 2002;248:307–318. [PubMed: 12167406]
42. Robu ME, et al. p53 activation by knockdown technologies. PLoS Genet 2007;3:e78. [PubMed: 17530925]
43. Nagel M, Tahinci E, Symes K, Winklbauer R. Guidance of mesoderm cell migration in the Xenopus gastrula requires PDGF signaling. Development 2004;131:2727–2736. [PubMed: 15128658]

44. Robu ME, et al. p53 activation by knockdown technologies. PLos Genetics 2007;3:e78. [PubMed: 17530925]

45. Walker MB, Kimmel CB. A two-color acid-free cartilage and bone stain for zebrafish larvae. Biotechnic and Histochemistry 2006;82:23–28. [PubMed: 17510811]

46. Ovcharenko I, Loots GG, Hardison RC, Miller W, Stubbs L. zPicture: dynamic alignment and visualization tool for analyzing conservation profiles. Genome Res 2004;14:472–477. [PubMed: 14993211]

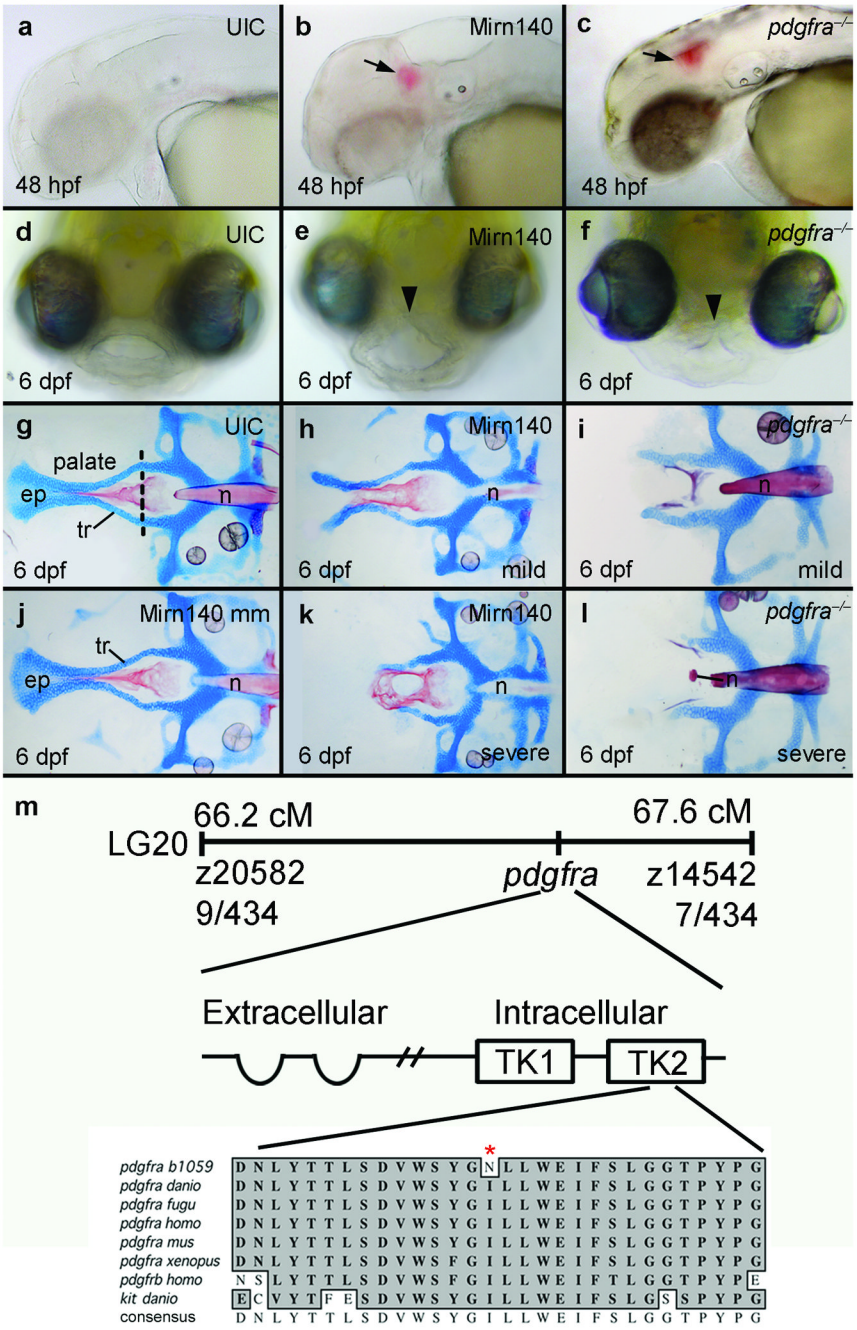

Figure 1.

Overexpression of Mirn140 phenocopies *pdgfra* mutants. (**a-c**) Animals injected with Mirn140 duplex had cranial hemorrhaging (arrows) at 48 hpf (**b**), mimicking the phenotype of zebrafish (**c**) and mouse *pdgfra* mutants[12,13]. (**d–f**) Frontal views of 6 dpf larvae show that, compared to uninjected controls (UIC) (**d**), Mirn140 duplex injected (**e**) and *pdgfra* mutant (**f**) animals develop hypoplastic upper lips (arrowheads). (**g–l**) In Alcian/Alizarin-stained palates of 6 dpf uninjected controls (UIC) (**g**) or Mirn140 mis-match control injected embryos (**j**) trabeculae (tr) fuse at the trabecular communis in the midline and extent anteriorly forming the ethmoid plate (ep), but Mirn140 duplex injected (**h,k**) and *pdgfra* mutants (**i,l**) show both mild (**h,i**) and severe (**k,l**) phenotypes that include complete clefting of the palatal skeleton. (**m**) The *b1059*

allele is a mutation of *pdgfrab*. *1059* was genetically mapped to linkage group 20 (LG20) between the polymorphic markers z20582 and z14542, with 9 cross-overs and 7 cross-overs, respectively, out of 434 meioses. Sequence analysis of wild-type and *b1059* mutant embryos revealed a missense mutation in the second tyrosine kinase (TK) domain of *pdgfra*. Protein sequence alignment of this region of the second tyrosine kinase domain (amino acids 841–870) of Pdgfra and related receptors shows the non-conservative I855N missense mutation (asterisk) in the second tyrosine kinase domain. This domain is highly conserved in Pdgfra across species as well as across related receptors such as Pdgfrb and Kit. n=notochord.

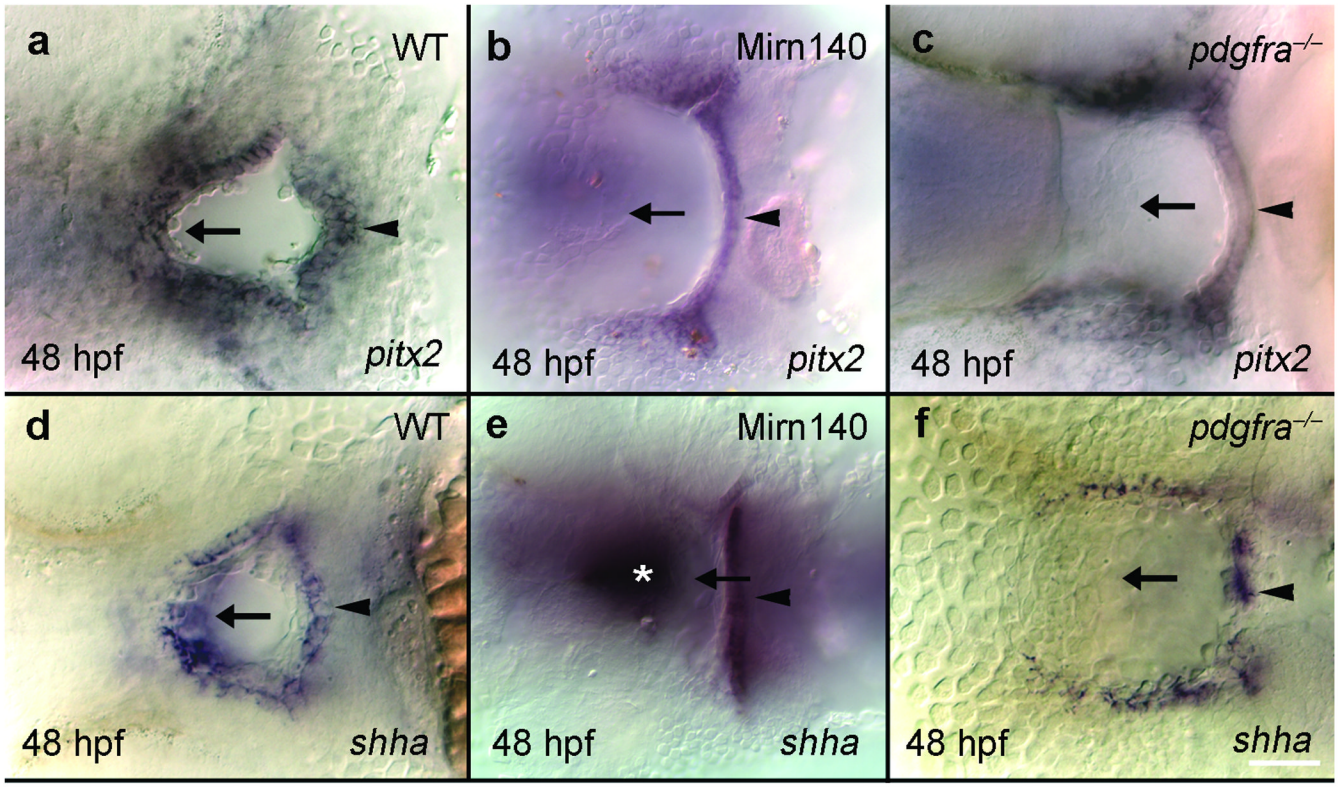

Figure 2.

The oral ectoderm is similarly disrupted in Mirn140 duplex injected embryos and *pdgfra* mutants. Ventral views, anterior to the left, of oral ectoderm labeled with *pitx2* (**a–c**) and *shha* (**d–f**) riboprobe in wild-type (**a,d**), Mirn140 duplex injected embryos (**b,e**) and *pdgfra* mutants (**c,f**). The roof of the oral ectoderm (arrows), adjacent to the normal location of palatal precursors, expressed neither gene in Mirn140 duplex injected embryos or *pdgfra* mutants. Loss of gene expression was specific to the roof of the oral ectoderm as the floor of the oral ectoderm expressed both *pitx2* and *shha* (arrowheads). The embryo in **e** is severely affected and *shha* staining in the ventral brain is evident (asterisk).

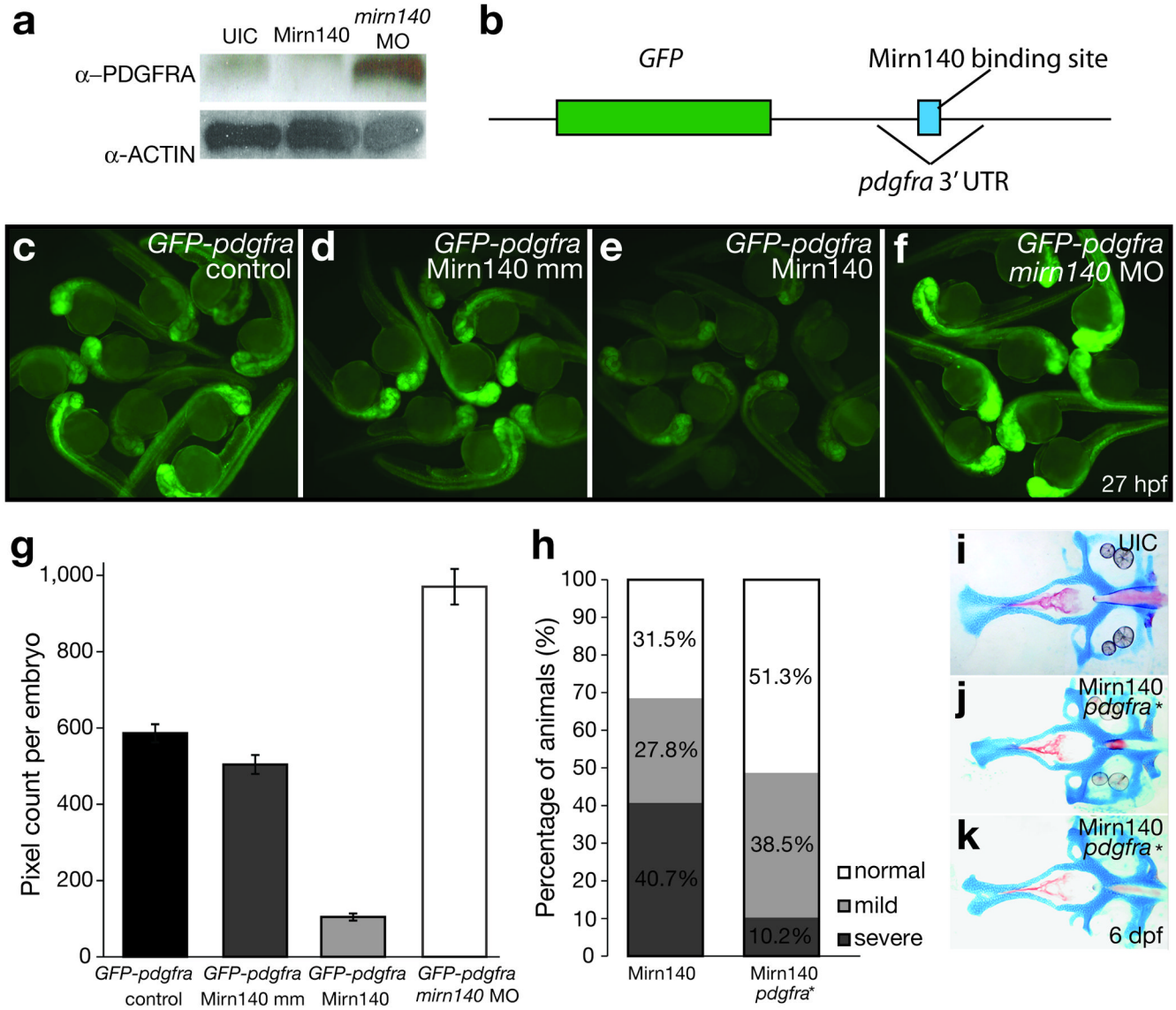

Figure 3.

Mirn140 regulates Pdgfra levels. (**a**) Compared to uninjected controls (UIC), Mirn140 duplex injection reduces and *mirn140* morpholino injection elevates the level of the endogenous Pdgfra protein, respectively, detected by anti-human PDGFRA antibody. Anti-mouse Actin antibody is used as a loading control. (**b**) Schematic of the *GFP-pdgfra* mRNA injected to test for interaction of Mirn140 with the *pdgfra* 3'UTR, which bears a predicted Mirn140 binding site. (**c–f**) 27 hpf embryos injected with *GFP-pdgfra* alone (**c**) or with *GFP-pdgfra* and Mirn140-mismatch (Mirn140mm) duplex (**d**) fluoresce more strongly than animals injected with *GFP-pdgfra* and Mirn140 duplex (**e**). Morpholino knockdown of Mirn140 with Dicer-inhibitor MO increased GFP fluorescence above controls (**f**). (**g**) Pixel density analysis of GFP fluorescence confirmed results of **c–f**; Error bars indicate standard deviations. (**h–k**) Synthetic *pdgfra* mRNA truncated to remove the Mirn140 binding site (*pdgfra**) rescued the cleft palate phenotype of Mirn140 over-expression, in three independent trials. (**h**) Distribution of palatal phenotypes after injection of Mirn140 duplex alone (n=54) or co-injection of Mirn140 and *pdgfra** mRNA (n=117), in percent of animals. Mildly affected fish had near normal trabeculae and lateral ethmoid plate, but lacked the medial ethmoid plate like Fig. 1m; and severely

affected fish lacked both the ethmoid plate and trabeculae like Fig. 1n. (**i–k**) Alizarin/Alcian-stained palates of 6 dpf uninjected control (UIC) (**i**) and co-injected embryos (**j, k**).

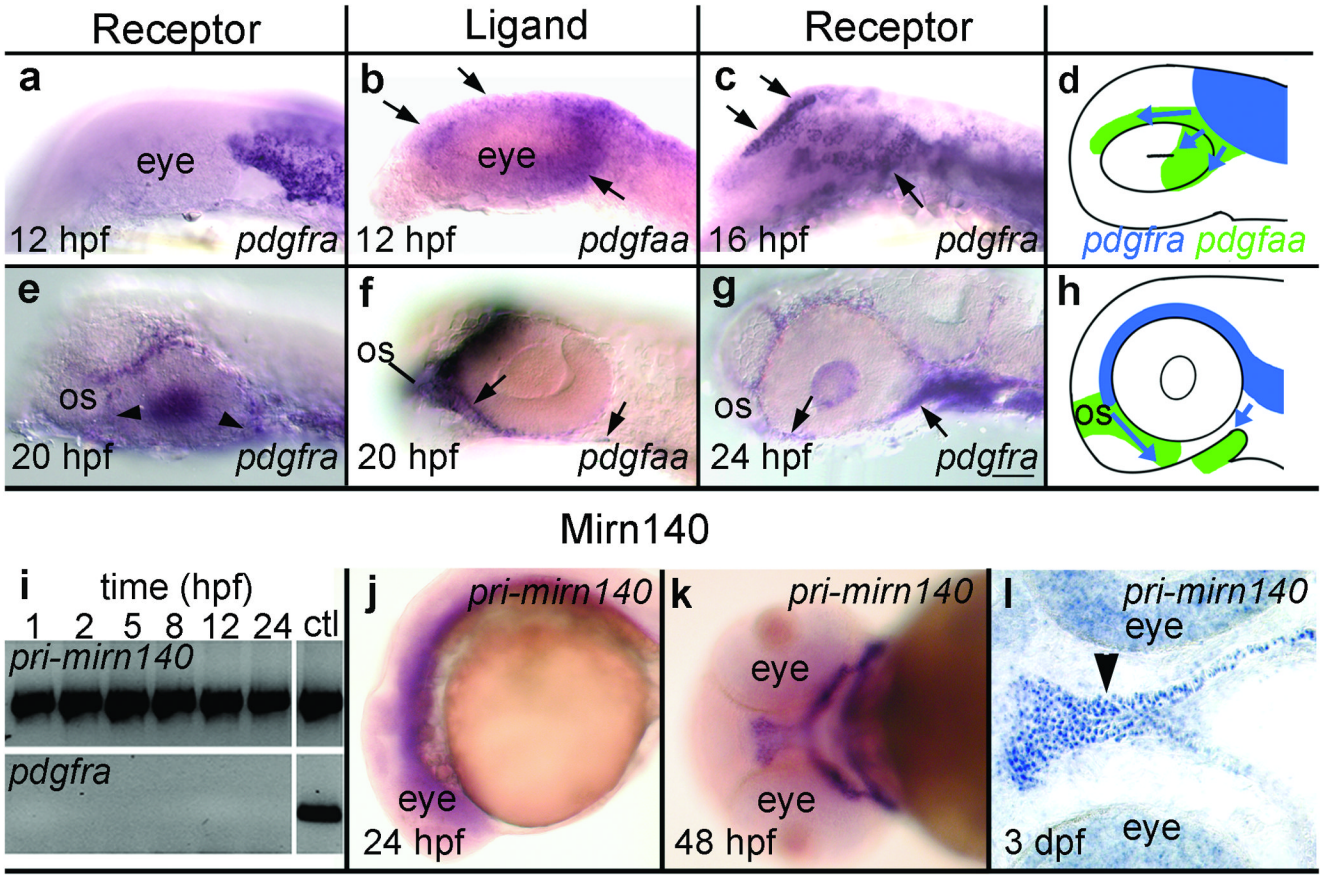

Figure 4.

mirn140 overlaps with *pdgfra* during crest cell migration. (**a–h**) *pdgfaa* expression predicts the migratory pathway of *pdgfra*-expressing crest cells. (**a–c**) Lateral views of *pdgfra* (**a,c**) or *pdgfaa* (**b**) expression in 12 hpf (**a,b**) and 16 hpf (**c**) embryos. Premigratory crest expresses *pdgfra* (**a**) while the midbrain rudiment expresses *pdgfaa* (**b**). By 16 hpf, the position of *pdgfra*-expressing crest cells (**c**) mirrors the 12 hpf distribution of *pdgfaa* (compare arrows in **b,c**). (**d**) Schematic of early crest cell migration (blue arrows) relative to 12 hpf *pdgfaa* expression (green). (**e-g**) Lateral views of 20 hpf (**e,f**) and 24 hpf (**g**) embryos stained with *pdgfra* (**e,g**) or *pdgfaa* (**f**) riboprobe. When *pdgfra*-expressing crest cells have migrated to the optic stalk (os) and are near the oral ectoderm (**e**, arrowheads) the optic stalk, oral ectoderm, and cells between these two tissues express *pdgfaa* (**f,** arrows). By 24 hpf, neural crest cells are condensing on the oral ectoderm (**g**, arrows). (**h**) Schematic depicting crest cell migration (blue, arrows) to the oral ectoderm relative to *pdgfaa* expression (green). (**i-l**) *mirn140* expression overlaps with *pdgfra*. (**i**) RT-PCR detects *mirn140* from one hpf onward. Controls for genomic contamination utilized primers targeted to intronic sequence and failed to yield PCR product except in PCRs utilizing genomic DNA (ctl) (**j-l**) *mirn140* transcripts detected by *pri-mirn140* riboprobe are broadly distributed during crest cell migration (**j**, lateral view) and become restricted to post-migratory crest cells (**k**, ventral view), including the palatal skeleton (**l**, arrowhead, horizontal section).

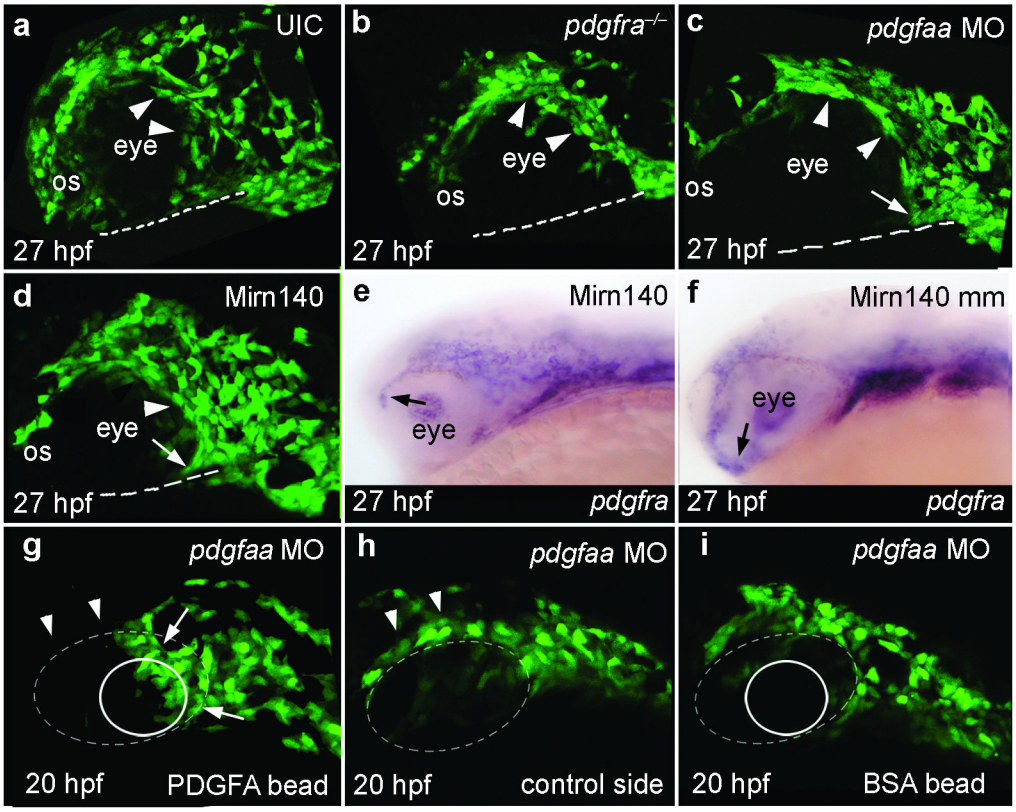

Figure 5.

Pdgf signaling, modulated by Mirn140, guides palatal skeleton precursors to the oral ectoderm. (**a–d**) Lateral views of 27 hpf *sox10:EGFP* transgenic embryos. (**a**) Neural crest cells disperse and migrate around the eye and optic stalk (os) to reach the oral ectoderm (dashed line) in uninjected control (UIC) embryos. (**b–d**) In contrast, most palatal precursor cells do not disperse (arrowheads) or migrate to the oral ectoderm in *pdgfra* mutants (**b**), *pdgfaa* morpholino injected embryos (**c**), or Mirn140 duplex injected embryos (**d**). In all three circumstances rostrally migrating crest cells stop migrating at the optic stalk. Caudally migrating crest is less severely effected in *pdgfaa* morpholino injected embryos and Mirn140 duplex injected embryos than in *pdgfra* mutants (arrows, **c,d,** see Supplementary Figure 5). (**e–f**) Lateral views of 27 hpf embryos stained with *pdgfra* riboprobe. *pdgfra* mRNA is similarly present in Mirn duplex (**e**) and mismatch control (**f**) injected embryos demonstrating that Mirn140's effect on migration is not through regulation of *pdgfra* transcripts. (**g–i**) Lateral views of *pdgfaa* morpholino injected (depleting endogenous Pdgfaa), *sox10:GFP* transgenic embryos implanted with rat recombinant PDGFA (**g,h**) or BSA (**i**) loaded beads (circles) just medial to the eye (dashed oval). (**g**) Crest cells accumulated adjacent to PDGFA beads (arrows, n=8) and fewer crest cells were present above the eye (arrowheads), compared to the control side of the same embryo (**h**) suggesting that crest cells were rerouted to the Pdgfa bead. (**i**) Control BSA beads did not attract crest cells.

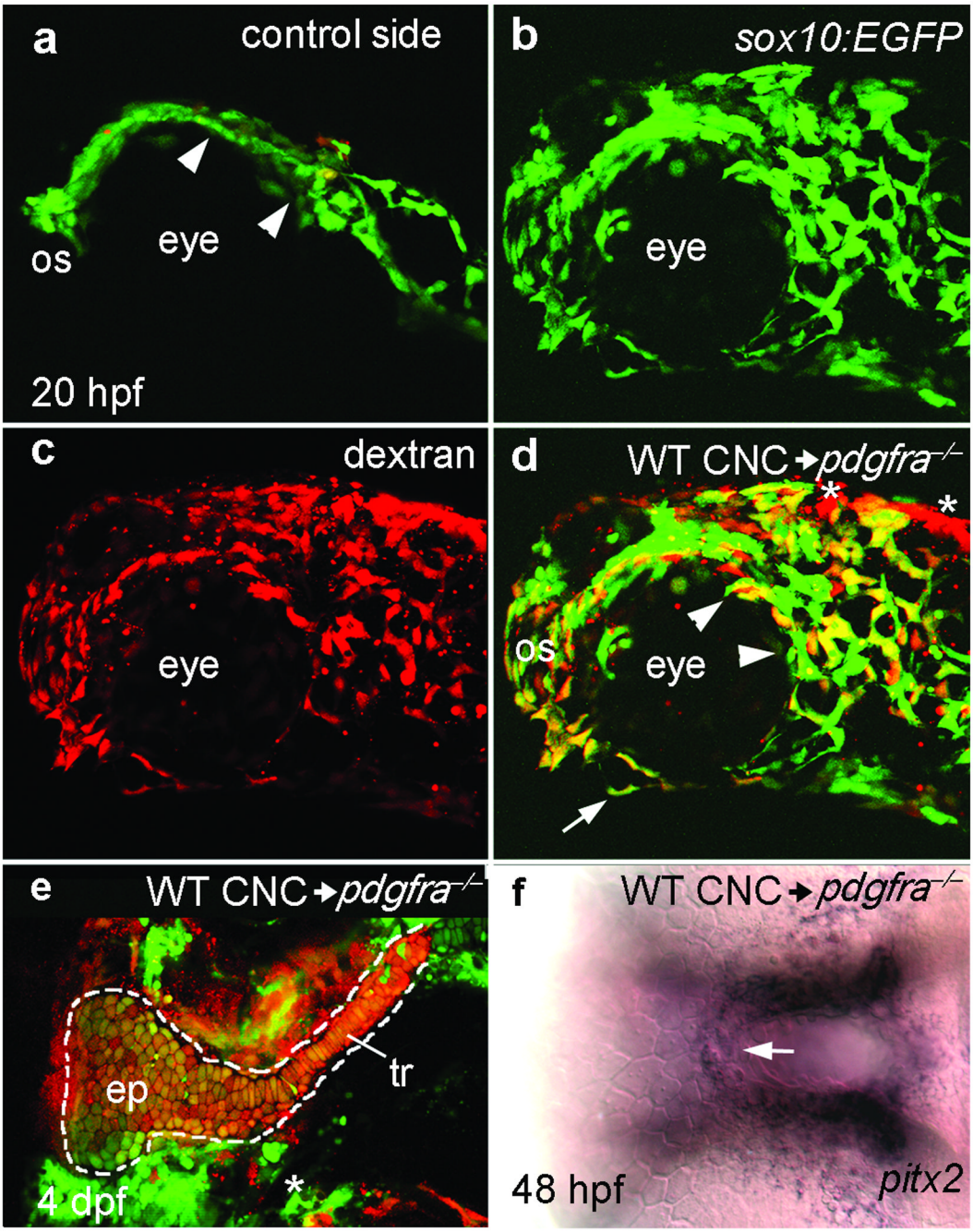

Figure 6.

Pdgfra is required in neural crest for neural crest cell migration, palatal skeleton development and proper oral ectoderm specification. (**a–d**) Lateral views of the control (**a**) and experimental side (**b–d**) of a 20 hpf *pdgfra* mutant embryo that received a neural crest cell transplantation from a *pdgfra*$^{+}$*;sox10:EGFP* embryo (WT CNC). (**a**) Mutant neural crest cells (green) are not dispersed (arrowheads) and failed to migrate beyond the optic stalk (os) on the side of the embryo that did not receive transplanted crest cells. (**b–d**) Donor *pdgfra*$^{+}$*;sox10*:EGFP transgenic cells, labeled with Alexa dextran 568 (**c**), have dispersed, migrated around the optic stalk, and reached the oral ectoderm (arrow in **d**) in a *pdgfra*$^{-/-}$ environment (n=21). (**d**) Merged imaged of **b,c**. Asterisks mark the location of two small patches of non-neural crest

cells in the transplant. (**e**) Flat mounted palatal skeleton of another *pdgfra* mutant that received a neural crest cell transplant from a *pdgfra*$^{+}$*;fli1*:EGFP transgenic donor (n=5). *pdgfra*$^{+}$ crest-derived cartilage was present unilaterally in the ethmoid plate (ep) and trabeculae (tr) of the palatal skeleton (outlined). The trabecula and a portion of the ethmoid plate on the control side of the mutant embryo host were missing (asterisk). (**f**) 48 hpf ventral view of the embryo in **a-d** showing *pdgfra*$^{+}$ crest rescues *pitx2* expression in the roof of the *pdgfra*$^{-/-}$ oral ectoderm (arrow, n=8). The contaminant cells, shown in **d**, are distant from the oral ectoderm and unlikely to influence oral ectodermal gene expression.

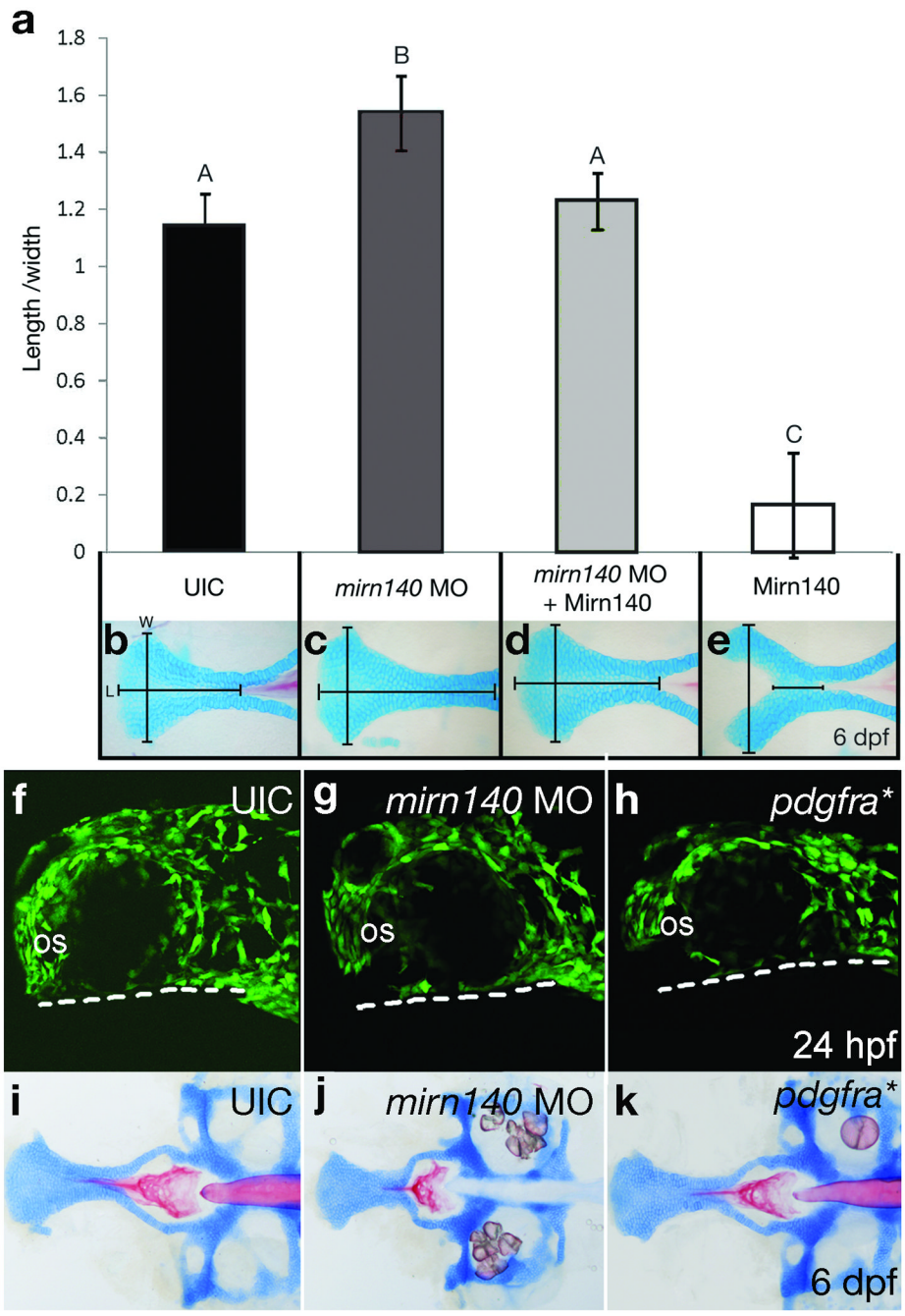

Figure 7.

Loss of Mirn140 function alters palatal skeleton morphology and neural crest cell migration. (**a–e**) At 6dpf the length-to-width ratio (as shown in **b–e**) was calculated in injected and control embryos. Compared to uninjected controls (UIC, n=9) and *mirn140* morpholino (MO) + Mirn140 duplex co-injected embryos (n=13), ratios were significantly larger and smaller in *mirn140* morpholino injected embryos (n=8) and Mirn140 duplex injected embryos (n=11), respectively. Levels not connected by the same letter are significantly different at the 0.05% level (Tukey-Kramer HSD; one-way ANOVA: $F_{1,57}$=186.7, p<0.0001). Error bars indicate standard deviation. (**f-h**) Compared to controls (**f,** n=8) fewer rostrally migrating neural crest cells had migrated from the optic stalk (os) to the oral ectoderm (dashed line) in

sox10:EGFP transgenic embryos injected with *mirn140* morpholino (**g**, n=10) or *pdgfra** mRNA (**h**, n=10). Neural crest cells did encircle the optic stalk in these embryos, unlike the effects of Pdgf loss-of-function (see Fig. 5). (**i–k**) The resultant palatal phenotypes in the same embryos imaged in **f–h**. Compared to controls (**i**) Palatal morphology was altered in *mirn140* morpholino injected embryos (**j**) but not *pdgfa** injected embryos (**k**).

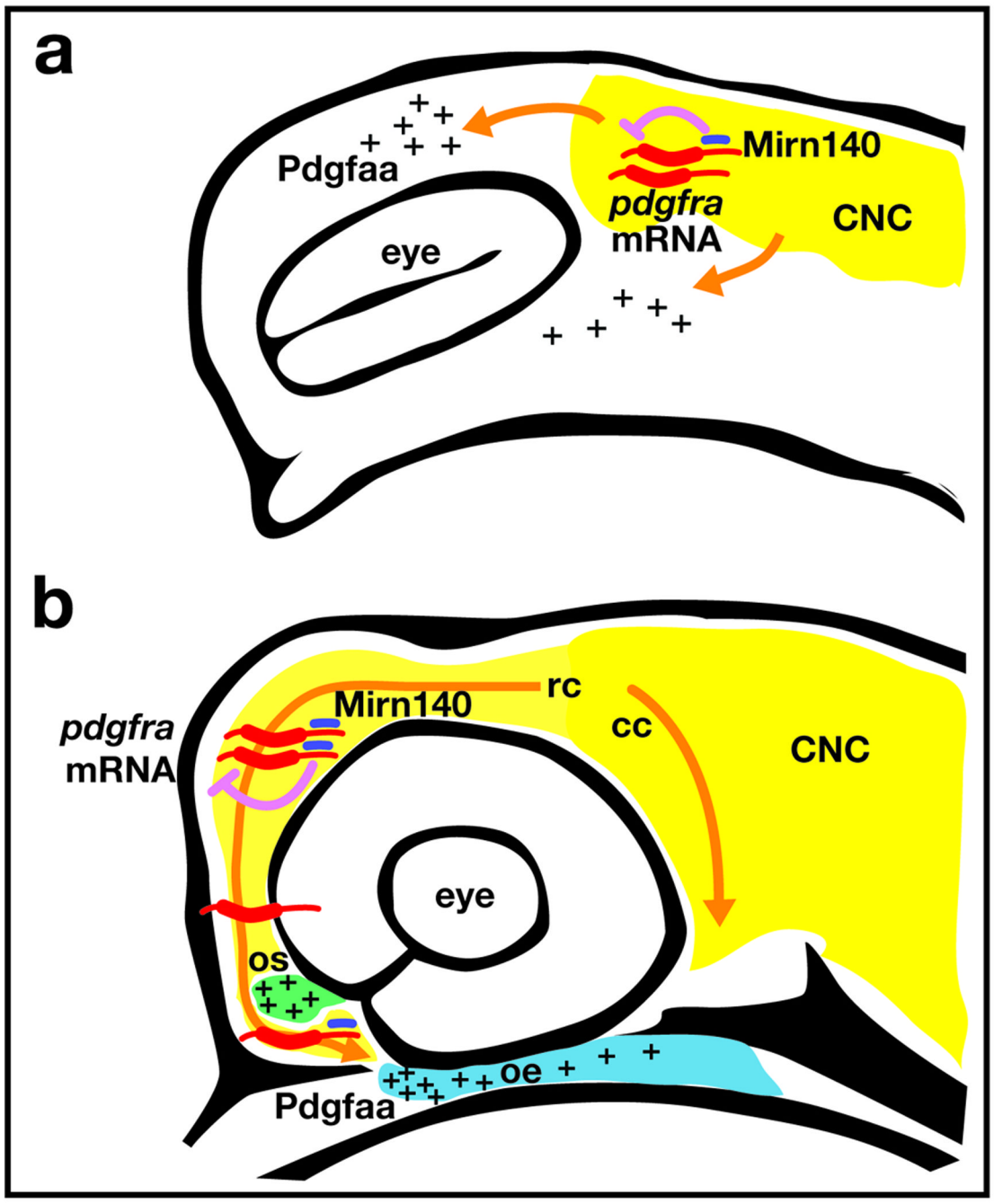

Figure 8.

Model of how Mirn140 modulates Pdgf signaling during palatogenesis. (**a**) Pdgfra signaling is required for neural crest cell dispersion. Neural crest cells (yellow) express *pdgfra* (red) and *mirn140* (blue) as they disperse into regions of *pdgfaa* expression (pluses). Mirn140 inhibits Pdgfra production (pink arrow), but the overall level of Pdgf signaling is sufficient to promote crest dispersion along Pdgfaa-positive pathways. (**b**) When rostrally migrating crest cells reach the optic stalk, stoichiometric differences in *pdgfra* and Mirn140 levels regulate their final migration. To envelope the optic stalk (green), crest cells require relatively higher levels of Pdgfra. Crest cells that migrate on towards the oral ectoderm (blue) must first decrease the levels of Pdgfra via Mirn140, in order to leave the optic stalk.